

Development of Control System for Atomic Tweezer Arrays

Submitted by:
Aditya Tripathi

Under the guidance of
Dr. Takeshi Fukuhara

January 29, 2024

Table of Contents

1 Introduction

- Background and Motivation

2 Estimation of tweezer potential (for Strontium Atoms)

- Basic Principles and Equations
- Plots for dipole potential and scattering rate

3 Optical Setup

4 Preparation of tweezer array beams

- Direct Digital Synthesis
- Homogenous power for each beam
- Results

Background, Motivation and Significance

Background and Motivation:

- It has been shown in recent years that individual precise control of atoms is possible using atomic tweezer arrays [1].

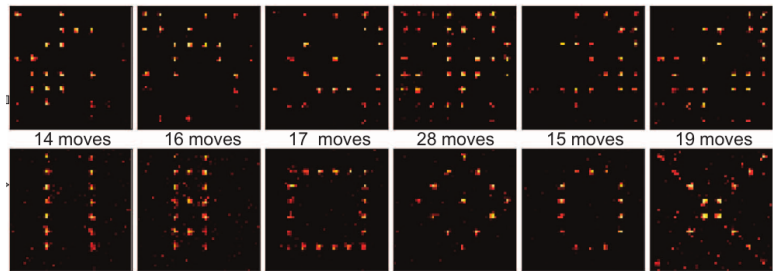


Figure: Gallery of fully loaded arrays

[1] Barredo, D., de Léséleuc, S., Lienhard, V., Lahaye, T., Browaeys, A., 2016. An atom-by-atom assembler of defect-free arbitrary two-dimensional atomic arrays. *Science* 354, 1021–1023.

Background, Motivation and Significance

Goal of my project:

- My project aimed to develop a control system that can be used to trap Strontium atoms.
- This project aims to understand atomic manipulation using optical methods, a field that stands at the forefront of modern quantum technologies.

Significance:

- Recently it was also shown [2] that a logical quantum processor can be made using reconfigurable atom arrays.
- This project can be extended to develop a quantum computing architecture using Strontium atoms.

[2] Bluvstein et. al. Logical quantum processor based on reconfigurable atom arrays

Gaussian Beam

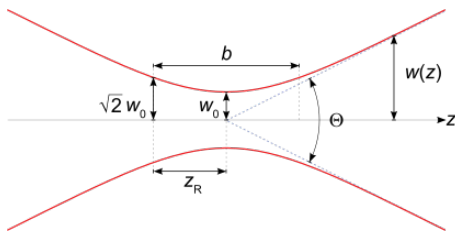


Figure: Gaussian Beam profile cross-section showing the variation of beam spot $w(z)$ [3]

The varying electric field for a gaussian beam is given by,

$$E(x, y, z) = \frac{E_0}{\sqrt{1 + (z/z_R)^2}} \exp\left(\frac{i k_0}{2\tilde{q}} (x^2 + y^2)\right) \exp(i [k_0 z - \psi])$$

where,

$$\tilde{q} = z - iz_R, \quad z_R = \frac{k_0 w_0^2}{2} = \frac{\pi w_0^2}{\lambda}, \quad \tan(\psi) = z/z_R$$

[3] Wiki, . URL: https://en.wikipedia.org/wiki/Gaussian_beam/media/File:GaussianBeamWaist.svg.

Basic Principles and Equations

- Laser light's intensity gradient induces a dipole force.
- Dipole potential results from atom polarization in the laser field.
- Atoms can be trapped in potential minima for red-detuned or maxima valleys for blue-detuned cases.
- Light-atom interaction causes photon scattering, limiting dipole atom trap performance.
- Semi-classical treatment is employed, assuming atoms as simple oscillators in a classical radiation field.

Basic Equations

The dipole potential is given by,

$$U_{dip}(\mathbf{r}) = -\frac{1}{2}\langle \mathbf{p}\mathbf{E} \rangle$$

The scattering rate is given by,

$$\Gamma_{sc}(\mathbf{r}) = \frac{P_{abs}}{\hbar\omega} = \frac{\langle \dot{\mathbf{p}}\mathbf{E} \rangle}{\hbar\omega}$$

Basic Equations

The final equations assuming the oscillator model
 $(\ddot{x} + \Gamma_\omega \dot{x} + \omega_0^2 x = -eE(t)/m_e)$ and ansatz for oscillating electric field are,

$$U_{\text{dip}}(\mathbf{r}) = -\frac{3\pi c^2}{2\omega_0^3} \left(\frac{\Gamma}{\omega_0 - \omega} + \frac{\Gamma}{\omega_0 + \omega} \right) I(\mathbf{r})$$

$$\Gamma_{sc}(\mathbf{r}) = \frac{3\pi c^2}{2\hbar\omega_0^3} \left(\frac{\omega}{\omega_0} \right)^3 \left(\frac{\Gamma}{\omega_0 - \omega} + \frac{\Gamma}{\omega_0 + \omega} \right)^2 I(\mathbf{r})$$

Here $\Gamma = \Gamma_\omega (\omega_0/\omega)^2$ is the on-resonance damping rate. On treating quantum mechanically, one gets,

$$\Delta E_i = \frac{3\pi c^2}{2\omega_0^3} \sum_{j \neq i} \frac{\Gamma_{ij}}{(\omega_i - \omega_j)} I(\vec{r})$$

For Sr atoms

$$U_{dip}(\vec{r}) = -\frac{3\pi c^2}{2} \left[\left(\frac{\Gamma_1}{\omega_{01} + \omega} + \frac{\Gamma_1}{\omega_{01} - \omega} \right) \frac{1}{\omega_{01}^3} + \left(\frac{\Gamma_2}{\omega_{02} + \omega} + \frac{\Gamma_2}{\omega_{02} - \omega} \right) \frac{1}{\omega_{02}^3} \right] I(\vec{r})$$

$$\Gamma_{sc}(\vec{r}) = \frac{3\pi c^2 \omega^3}{2\hbar} \left[\left(\frac{\Gamma_1}{\omega_{01} + \omega} + \frac{\Gamma_1}{\omega_{01} - \omega} \right)^2 \frac{1}{\omega_{01}^6} + \left(\frac{\Gamma_2}{\omega_{02} + \omega} + \frac{\Gamma_2}{\omega_{02} - \omega} \right)^2 \frac{1}{\omega_{02}^6} \right] I(\vec{r})$$

where Γ_1 and Γ_2 are the line widths for $5s^2 \ ^1S_0 \rightarrow 5s5p \ ^1P_1$ and $5s^2 \ ^1S_0 \rightarrow 5s5p \ ^3P_1$, and ω_{0i} is the respective energy difference of the level divided by \hbar .

Level scheme for Strontium

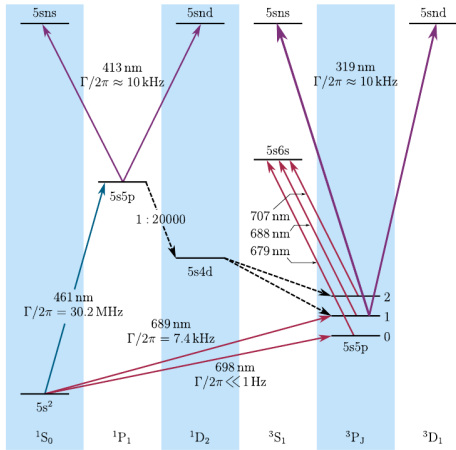


Figure: Level scheme of Strontium atoms [4]

[4] HANLEY, R., 2018. Creation of a strontium microtrap: Towards a spin-squeezed atomic clock.

Plots for dipole potential and scattering rate

Assumptions: The power of the laser is 0.025W and the beam waist(ω_0) for the Gaussian beam profile is $1\mu m$.

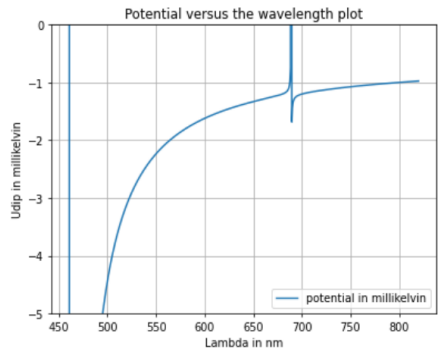


Figure: Dipole potential vs Wavelength

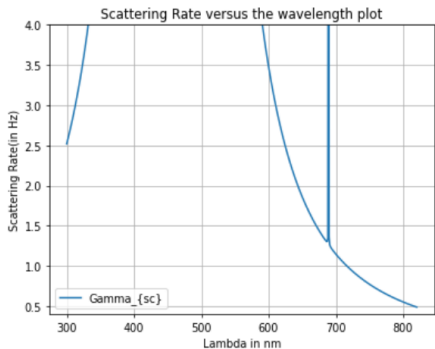


Figure: Scattering rate vs Wavelength

Rough estimates

The wavelength used in the setup is 813 nm. This is the magic wavelength at this wavelength it is found that the scattering rate is $\approx 0.5\text{Hz}$ and $\mathbf{U}_{\text{dip}}/\mathbf{k_b} = 1\text{mK}$. The intensity profile for a Gaussian beam is given by,

$$I(r, z) = \frac{2P}{\pi w_0^2} \exp\left(-2\frac{r^2}{w^2(z)}\right)$$

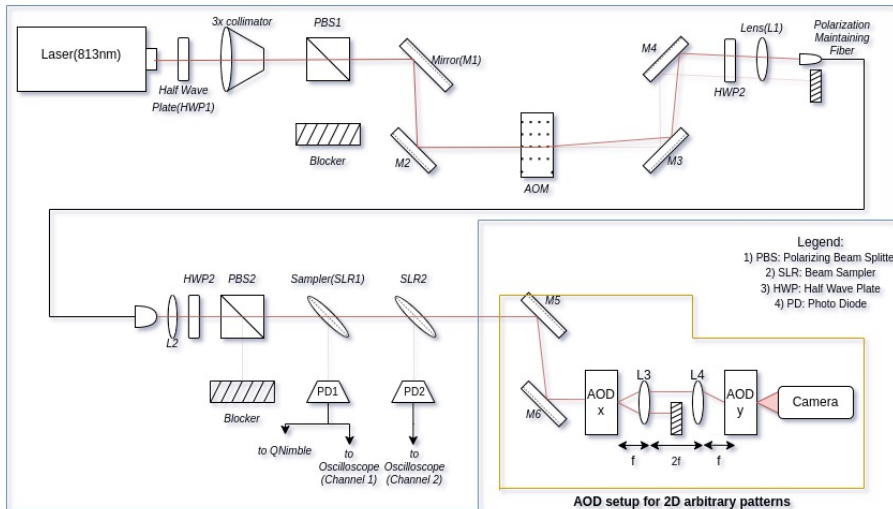
The above can be approximated to a quadratic potential which in turn gives us the radial and axial trapping frequencies.

$$\omega_r = (4\hat{U}/m\omega_0^2)^{1/2}, \quad \omega_z = (2\hat{U}/mz_R^2)^{1/2}$$

For the depth of 1mK and, beam waist $1\mu\text{m}$, and the mass of Sr atoms, we get the approximate values,

$$\omega_r \approx 600 \text{ kHz} ; \quad \omega_z \approx 100 \text{ kHz}$$

Optical Setup



Beam intensity stabilization

Figure: Schematic for the optical setup

Optical Setup

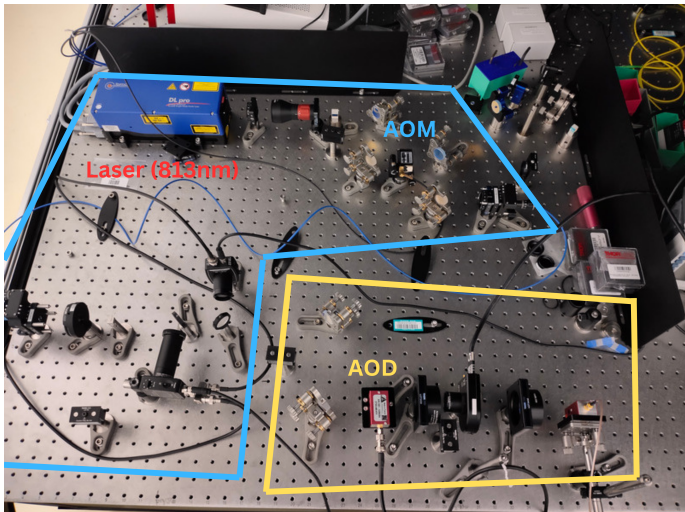


Figure: Setup on the optical bench

Intensity Stabilization

- The Acousto optic modulator (AOM) working with the PID (Proportional, Integral, and Differential) feedback provides control over the laser intensity.
- AOMs work on creating diffraction grating of sinusoidal refractive index in a crystal using radio frequency acoustic waves generated by a transducer attached to the end of the crystal.
- The angle at which laser enters AOM is optimized to get the maximum diffraction efficiency.

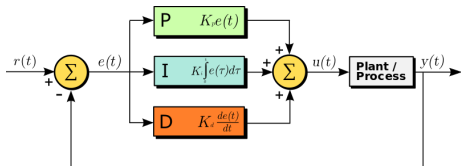


Figure: Block Diagram for PID control

Acousto-optic Deflector (AOD)

- AOD is a device primarily used to deflect the path of a laser beam.
- Compared to AOM, AOD produces a large deflection angle.
- AOD is primarily used for beam steering while AOM is used for intensity stabilization purposes.

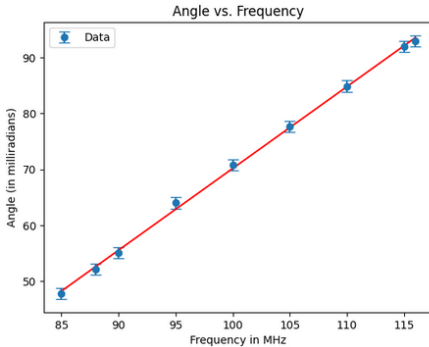


Figure: Deflection angle vs Frequency (slope=0.084 ± 0.003 degrees per MHz)

- The frequency range of operation is from 85.5 MHz to 121.5 MHz.
- Using the value of beam divergence in the x and y direction the resolution can be found.
- Using the resolution in the x-direction the maximum possible traps come out to be 23 ± 4 and in the y-direction, it is 52 ± 6 .
- The beam is not perfectly circular. The use of an appropriate lens will correct the beam mode.
- To obtain the figure in the previous slide a Signal Generator was used.

Can we automate the process of signal generation?

Direct Digital Synthesis Theory

- DDS is used to generate high frequencies of the order of 100s of MHz.
- To do so DDS architecture requires the input of a precise reference clock, a programmable read-only memory (PROM), and a Digital to Analog Converter.

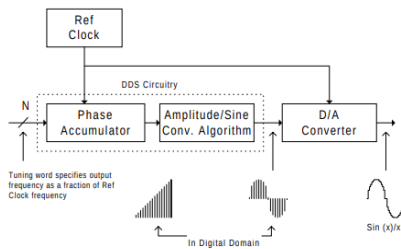


Figure: DDS flowchart with Phase Accumulator [5]

- The output frequency is given by, $f_{\text{out}} = \frac{(ftw)(f_s)}{2^N}$

[5] Analog Devices. A technical tutorial on digital signal synthesis.

AD9959 Eval Board with Raspberry Pi Pico

- To change frequency quickly RPi is coupled with the Eval Board of AD9959.
- The communication between RPi and AD9959 is via SPI. Speed was found to be roughly 54 kilobytes/second. Frequency and Amplitude together take up a 7-byte transfer. Thus the speed of switching between 2 arbitrary frequencies with different amplitudes is roughly 7-8 kHz.

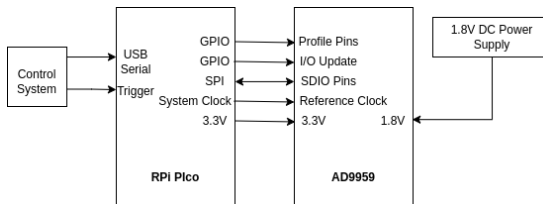


Figure: Block wiring diagram for DDS with RPi Pico

Homogenous power output for each beam

- Changing the frequency changes the diffraction angle for AOD which changes the diffraction efficiency
- Changing the power input (V_{rms}) to AOD of the high frequencies can also change the diffraction efficiency

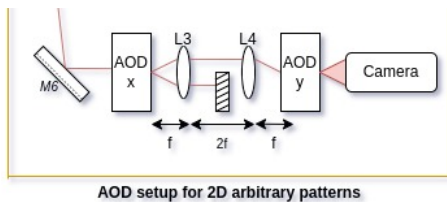


Figure: AOD setup

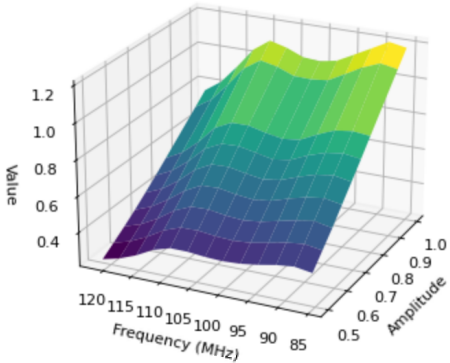


Figure: Plot of 1st Diffracted Beam Power for different Frequencies and Amplitudes (Amplitudes are scaled to 1) (Photodiode value is in Volts)

Result of Stabilization

Six frequencies were taken from 85.5 to 120.5 MHz. Then from the contour, their respective amplitude were sent to DDS, to get a stable power output.

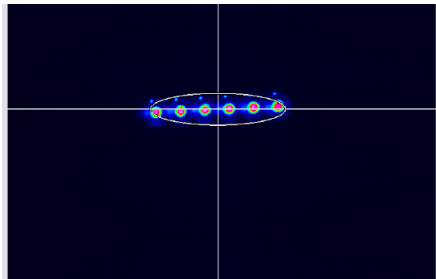


Figure: Fast switching between 6 frequencies (exposure time is 12ms)

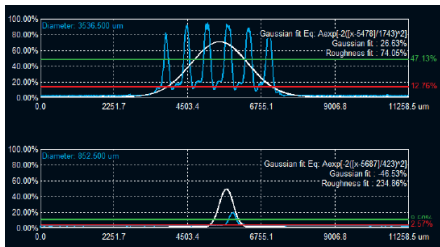


Figure: Cross-section of the left figure

Problem in Stabilization

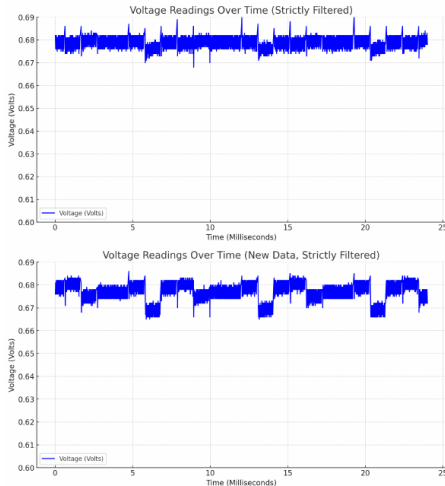


Figure: Output from photodiode. The two plots were taken 25 minutes apart

Conclusion

- To get a stabilized power output a table of 6 pairs of frequency and amplitude was programmed.
- However it was seen that over long time intervals, the output became destabilized (the percentage deviation increased from 0.49% to 0.68 %)
- The reason for the above is still to be investigated.
- To get 2-d patterns we need to put an AOD in the perpendicular direction.

2-d Patterns

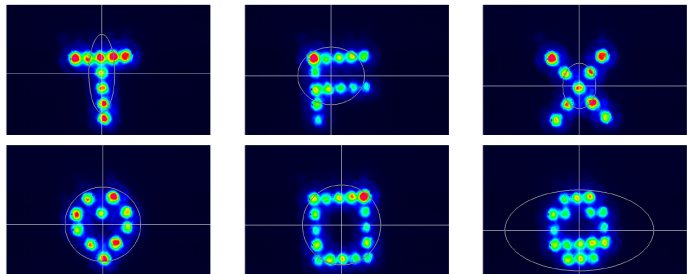


Figure: Some 2-D Patterns generated after the Second AOD

- Inhomogeneity in beam power attributed to the unoptimized 2nd AOD

Future Prospects

- Speed Constraints: Average switching time, 0.1 to 1 millisecond. Limitations attributed to RF generation setup; potential for improvement with a more efficient algorithm and faster SPI communication architecture.
- Intensity Profile: Achieved stable beam intensity profiles for six beams using a frequency and amplitude table.
- Feedback after AOD: Instead of a table, feedback may provide better results.
- Additional cooling setup required (e.g. MOT) to bring down the temperature to a few milliKelvins. Then the cloud of Sr atoms can be further cooled and trapped using the current setup.

Neutral-atom quantum computer in action

Bluvstein et. al. Logical quantum processor based on reconfigurable atom arrays

Acknowledgement

I would like to thank Dr. Takeshi Fukuhara for hosting me in his lab at Riken and also for being a very kind and supportive supervisor. I would also like to thank Dr. Yamamoto, Dr. Ozawa, and Kizaki-san for their support. I would sincerely like to thank all my friends and mentors at CBS.